Increasing Trend of Precipitable Water Vapor in Antarctica and Greenland

Junsheng Ding[1,2], Junping Chen[1,2(✉)], and Wenjie Tang[1,2]

[1] Shanghai Astronomical Observatory, Chinese Academy of Sciences, Shanghai 200030, China
{dingjunsheng, junping}@shao.ac.cn
[2] University of Chinese Academy of Sciences, Beijing 100049, China

Abstract. Polar precipitable water vapor (PWV) is expected to increase under a warming climate. However, the conventional approach cannot provide sufficient long-term PWV records due to the high maintenance costs. Fortunately, the exponential explosion in the number of geodetic-quality Global Navigation Satellite System (GNSS) stations has broken this deadlock. Utilizing radiosonde and GNSS data over two decades (1994–2020), we analyzed and evaluated the spatial and temporal variability characteristics of PWV in Antarctica and Greenland. The multi-year mean PWV values for Antarctica and Greenland were 5.63 ± 1.67 mms and 7.63 ± 1.35 mms, respectively, with annual standard deviations (STD) of PWV of 1.60 ± 0.77 mms and 3.44 ± 0.92 mms, respectively. In both Antarctica and Greenland, the PWV annual STD shows a gradual increase from the land center to the edge; while the PWV mean decreases with increasing latitude in Greenland, there is no significant latitudinal correlation in Antarctica. There is no significant regional difference in PWV trends, and from the statistical results, both Antarctica and Greenland show an increasing trend from year to year. The PWV trends in Antarctica and Greenland were 0.29 ± 0.77 mm/decade and 0.27 ± 0.64 mm/decade, respectively, with relative PWV trends of 5.98 ± 12.93%/decade and 3.87 ± 8.45%/decade, respectively.

Keywords: Precipitable water vapor · GNSS · Radiosonde · Antarctica and Greenland

1 Introduction

Water vapour affects the Earth's radiative balance by absorbing long-wave radiation and its latent heat of phase change can alter atmospheric circulation, providing the greatest positive feedback on global warming and is the most important greenhouse gas [1–5]. In addition, in the context of global climate change, the frequency of extreme precipitation has increased, which has severely affected the environment and human production and life [6–11]. Monitoring the variation of water vapour is thus significant for the global energy cycle and understanding global warming but also for monitoring climate change and safeguarding human life and property.

Considering the warmer atmosphere and more open sea water, it is expected that the PWV of polar region will increase accordingly, which will be thought as feedback

© Aerospace Information Research Institute 2022
C. Yang and J. Xie (Eds.): *China Satellite Navigation Conference (CSNC 2022) Proceedings*, LNEE 908, pp. 286–296, 2022.
https://doi.org/10.1007/978-981-19-2588-7_27

for further warming [12]. Yet, there are few studies related to the spatial and temporal characterization of PWV in the polar regions, due to observational difficulties. The previous methods to obtain PWV can be classified into two categories. The first category of method is the reanalysis dataset, it is produced by assimilating various types of observations into dynamic coherent data sets based on atmospheric circulation models [13, 14]. Data obtained by this category have the advantages of global coverage, spatial integrity and homogeneous record, but reanalysis data may be less reliable for areas where no or limited data assimilation observations are available [4, 15]. Another category is observations directly measured from various sensors such as weather stations, satellite remote sensing, radiosonde and Global Navigation Satellite System (GNSS). The advantage of these methods is the high accuracy of the measurements obtained at each station, but it is often difficult to analyze long-term PWV variations due to incomplete observations, sparse and non-uniform global distribution [16, 17].

Fortunately, with the rapid development of GNSS in recent years, the number of ground-based GNSS stations and the data obtained by these stations have also exploded [18, 19]. Ground-based GNSS observations are inexpensive to build and maintain, and once the equipment is deployed, it can be used directly for observation without calibration and correction, enabling large-scale, high-density networking [20, 21]. The accuracy of the observations is not affected by weather changes, so it is possible to continuously monitor PWV with high accuracy under various adverse weather conditions, and its time resolution can meet the needs of many meteorological studies. Especially in the polar regions, the emergence of a large number of GNSS stations makes it possible to analyze the time and space changes of the polar high-precision PWV.

Here, we have extracted and analyzed the spatial and temporal characteristics of the PWVs for Antarctica and Greenland using GNSS PWVs from the Nevada Geodetic Laboratory (NGL) and radiosonde PWVs from IGRA2 (Integrated Global Radiosonde Archive V2). The data span the period 1994–2020 and possible systematic offsets between the two types of data have been corrected for by co-locating the stations. The structure of this paper is as follows: In Sect. 1, the significance of PWV and the current research status of polar PWV are introduced. Section 2 describes the assessment data and methods. In Sect. 3, the assessment results are presented and the temporal and spatial distribution characteristics of the polar PWV are analyzed. Section 4 gives the conclusions.

2 Data

2.1 Radiosonde and GNSS PWV

In this study, polar radiosonde (RS) and GNSS data are obtained from the IGRA2 (ftp://ftp.ncdc.noaa.gov/pub/data/igra/) and NGL (http://geodesy.unr.edu/), respectively. Limited by the fact that the earliest GNSS record in the database is 1994, we truncated the radiosonde data before 1994 as well to keep the consistency between the two types of data. In addition, some sites with poor data quality, insufficient data record length, jumps in data records, or significant manmade deviations were excluded.

Figure 1 shows the distribution of the selected sites in Antarctica and Greenland. In Antarctica, there are 12 stations belonging to IGRA2 and 55 stations belonging to NGL; in Greenland, there are 8 stations belonging to IGRA2 and 50 stations belonging to NGL.

The color bar in Fig. 1 represents the height, from which it can be found that both in Antarctica and Greenland, the RS stations are almost all located in the low height land edge region (AMU2 height is 2835 m and the rest of the stations have an average height of 36 m; SMM2 station height is 3255 m and the rest of the stations have an average height of 51 m), while the addition of GNSS stations (GNSS stations in Antarctica and Greenland mean elevations of 970 m and 711 m, respectively) has changed this state considerably, that is, it has enriched the PWV record in the polar region not only in plane but also in height.

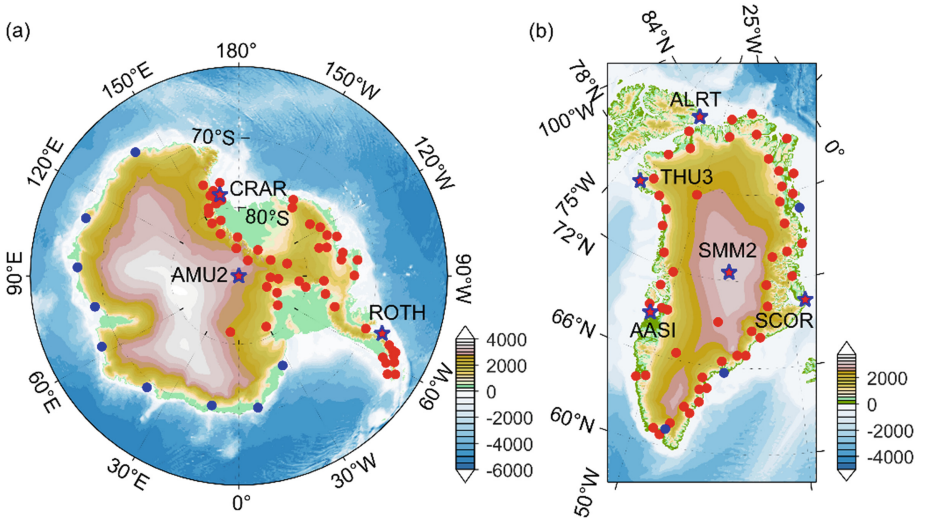

Fig. 1. GNSS (red dots) and radiosonde (blue dots) sites on Antarctica (left) and Greenland (right). The location of the pentagrams with blue edges has both GNSS and RS site, some of them are selected for comparing PWV (Fig. 2). The color bar represents the height in meters.

2.2 PWV Comparison and Assimilation

Most of the RS and GNSS stations do not overlap, but there are still a small number of co-located stations (Fig. 1, pentagrams with blue edges), with three pairs in Antarctica and five pairs in Greenland. The PWVs of these stations were used to compare the differences between the two types of data and then assimilated.

Since the temporal resolution of GNSS data is 5 min, and RS has only two observations a day, time matching was performed first. In the time matching, GNSS observations at the same moment as the RS observations are retained, while for GNSS observations that cannot be strictly matched at the moment, the average value of the corresponding hour is used as a substitute.

Figure 2 illustrates the comparison of two types of PWV data from four sites AMU2, CRAR, SMM2 and AASI, they represent the central and marginal regions of Greenland, Antarctica, respectively. Among these station pairs, AMU2, located in the center of Antarctica, has very small PWV and almost no periodic properties due to its high latitude and altitude, and the correlation coefficients between the two types of observations are much smaller than those of the other stations. The correlation coefficients of the other stations are greater than 0.9 and the RMSE are within 2 mm. Although it is very small, it still indicates that there is a systematic difference between the PWVs obtained in these two ways, and this error needs to be removed when the two data are used together in the analysis. Therefore, we assimilated the PWV of the surrounding GNSS stations to the RS PWV based on the mean bias of these co-located stations. The assimilation is done by adding the monthly mean deviation from the GNSS to the RS observations, with the reference station being the closest latitudinal co-located station.

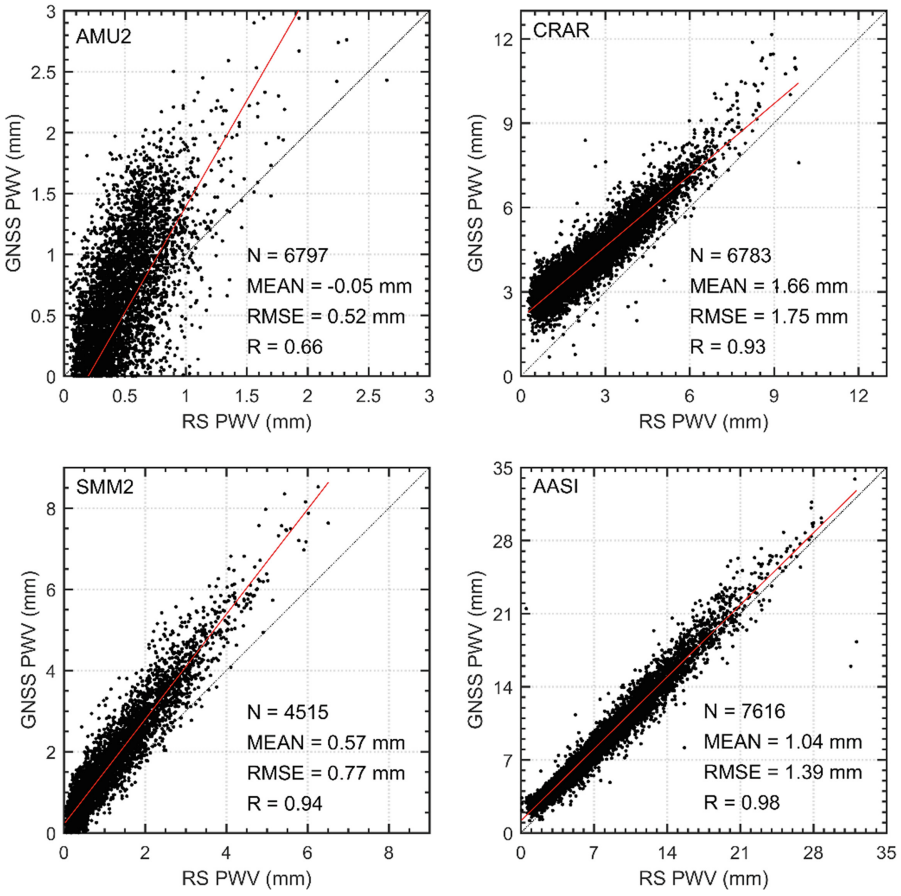

Fig. 2. Comparison of two types of PWV data from four sites AMU2, CRAR, SMM2 and AASI. N represents the number of points and R represents the correlation coefficient. The red line represents the fitting line between RS PWV and GNSS PWV.

3 Results and Discussion

The annual means and standard deviations of RS PWV and assimilated GNSS PWV at each site are calculated and counted, and the multi-year averages of these site means and standard deviations are calculated and analyzed, in addition to the growth rates of the annual means. The spatial distribution of these data in Antarctica and Greenland is described and discussed in this section.

3.1 Mean and Standard Deviation

The mean value represents the overall annual PWV level at the location of the station, while the standard deviation represents the sharpness of PWV fluctuations within a year at that location. Since the PWV mean is influenced by both latitude and height, we first impute the PWV mean of all stations to the ellipsoidal height according to the exponential model, that is, the ellipsoidal height of the imputed PWV is all zero. The exponential model is built based on the PWV mean and ellipsoidal height of all stations in the region. In Antarctica and Greenland, the zero-height value of the exponential model is 5.548 and 7.599, respectively, and the natural exponential index is -9.541×104 and -4.764×104, respectively. This also indicates that Greenland is at a lower latitude than Antarctica (which is also the fact) and that PWV decreases faster with height in Antarctica than in Greenland.

After the processing described above, the PWV means and standard deviations are plotted in Fig. 3. Subplots (a) and (b) of Fig. 3 show the mean PWV values for Antarctica and Greenland, respectively. From subplot (a), it can be found that the overall mean PWV values in Antarctica are in the range of 2–9 mm, with the larger values larger than 7 mm basically concentrated in the lower latitude Antarctic Peninsula region, while the smaller values smaller than 5 mm are mostly in Queen Maud Land and Wilkes Land (actually the land edge of these two regions). In contrast, the distribution of the mean PWV values in the Ross Ice Shelf, Lonnie Ice Shelf and West Antarctica regions spans a wide range of values and is not concentrated in a single value. Subplot (b) shows the mean PWV values for Greenland Island, these values are in the range of 5–10 mm. From subplot (b), it is obvious that the PWV decreases with increasing latitude. In addition, the contour lines show that Greenland Island as a whole resembles a "flat-topped mountain", i.e., the elevation climbs expressly at the edge of the island and slows down at the center of the island. From the stations at the same latitude, the PWV is higher at the edge of the island, away from the ocean, than near the ocean, while the PWV is not higher at the center of the island, even though the station is farther away from the ocean.

Subplots (c) and (d) of Fig. 3 show the standard deviation of PWV for Antarctica and Greenland Island, respectively, with the standard deviation ranging from 0–3 mm for Antarctica and from 1–6 mm for Greenland. It can be significantly found that in Antarctica, the standard deviation of PWV decreases with increasing latitude, while the standard deviation of PWV in Greenland does not vary significantly with dimension, but it can be found significantly that the further away from the coastline, the smaller the

standard deviation of PWV is, with the smallest standard deviation occurring in the center of Greenland, while the largest standard deviation occurs in the coastal area at the southern end of Greenland.

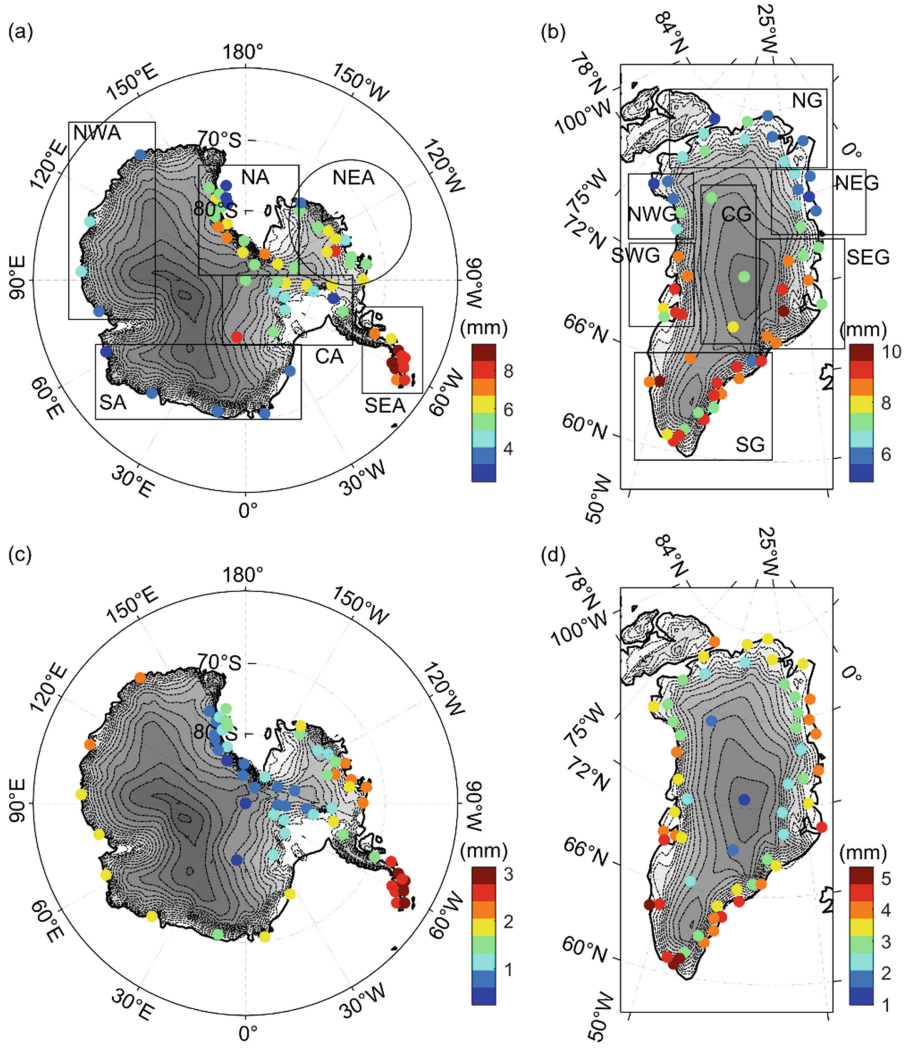

Fig. 3. Annual mean PWV (a)(b) and standard deviation PWV (c)(d) of Antarctica (left) and Greenland (right). (NWA = northwestern Antarctica, NA = northern Antarctica, NEA = northeastern Antarctica, CA = center Antarctica, SEA = southeastern Antarctica, SA = southern Antarctica; NG = northern Greenland, NWG = northwestern Greenland, NEG = northeastern Greenland, SWG = southwestern Greenland, CG = center Greenland, SEG = southeastern Greenland, SG = south Greenland, it should be noted that the above orientation refers to the picture rather than the actual orientation).

From the above analysis and discussion, it is also found that the PWV mean and standard deviation are relatively stable in the region, so we divided all stations into regions according to the values and location of PWV. The results of the regional division are shown in subplots (a) and (b) of Fig. 3. The stations in each box (or circle) are divided into a group, and the names of the regions are also marked in the figure. It is important to note that the region naming here is based on the orientation in the figure and does not represent the actual orientation.

After grouping, the PWV mean and standard deviation were calculated for each region and the results are displayed in Fig. 4. The left side of the red dashed line in Fig. 4 shows the six subdivisions in Antarctica, and the right side shows the seven subdivisions in Greenland Island. Combining subplots (a) and (b) of Fig. 4 and Fig. 3, it can be found that: (1) The mean values of PWV in the NA and CA regions of Antarctica, which are on the ice shelf, are not low but the regional STD is the smallest among all regions. (2) The STD of the NEA region, which is similar in location but different in orientation, is basically the same as that of NWA and SA, but the mean value is significantly larger than the latter two. (3) The mean value of CG in the central region of Greenland is not significantly different from other regions, but the STD is the smallest among all regions. (4) The three regions in the south of Greenland, SWG, SEG and SG, have no significant difference in mean values, but the STD is SG > SWG > SEG.

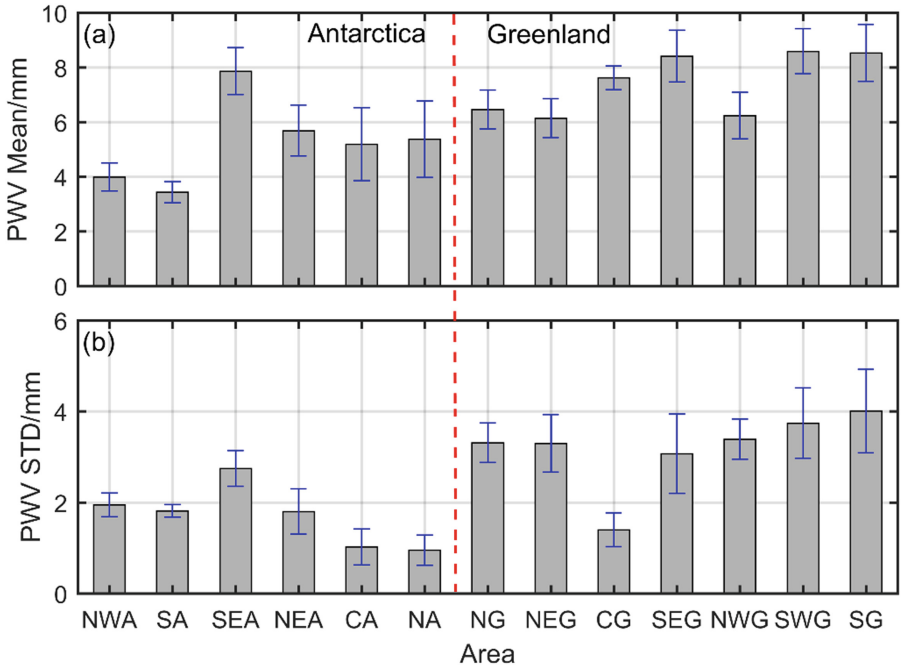

Fig. 4. (a) PWV mean and (b) PWV standard deviation in each area of Antarctica and Greenland. The blue error bars indicate the standard deviation of the mean.

3.2 Interannual Variation

The mean and STD reflect the average state over many years, while the annual growth rate can reflect the interannual variation. After obtaining the PWV mean for each station for each year, the linear trend of each station is calculated. Considering the large differences in PWV mean between stations, the relative liner trend is more representative of the interannual variation of the stations, so the relative liner trend (the ratio of linear trend to PWV mean) is also calculated, and they are plotted in Fig. 5.

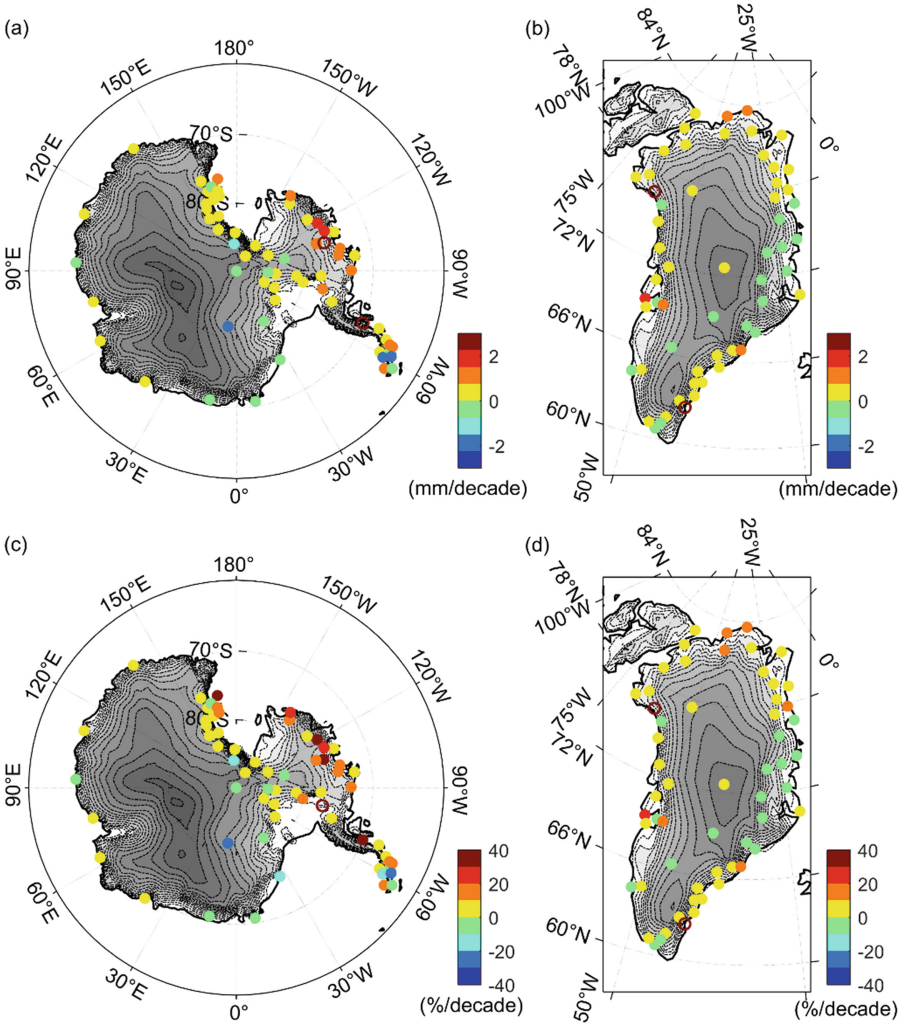

Fig. 5. (a) and (b) Spatial pattern of PWV trends during 1994–2020, (c) and (d) spatial pattern of PWV trend rates during 1994–2020. Filled circles indicate that the trends are statistically significant at the 95% confidence level.

Subplots (a) and (c) of Fig. 5 show the linear and relative linear trends in Antarctica. Combining these two subplots, it can be found that (1) the linear trends of the vast majority of stations are within ±1 mm/decade, and the number of stations with positive values is significantly more than those with negative values; (2) except for some stations in the NEA and NA regions, the relative linear trends of the vast majority of stations are consistent with the linear trends; (3) The linear trend is larger for stations in the NEA region than in the other regions.

Subplots (b) and (d) of Fig. 5 show the linear and relative linear trends for Greenland Island, and the combination of these two subplots shows that: (1) like Antarctica, the linear trend of PWV in Greenland Island is also mostly within ±1 mm/decade, and more stations have positive values than negative ones, but it is less significant than in Antarctica; (2) the stations with the negative linear trend are mainly located in the eastern part of Greenland and the saddle; (3) the relative linear trend is smoother than the linear trend among the regional stations.

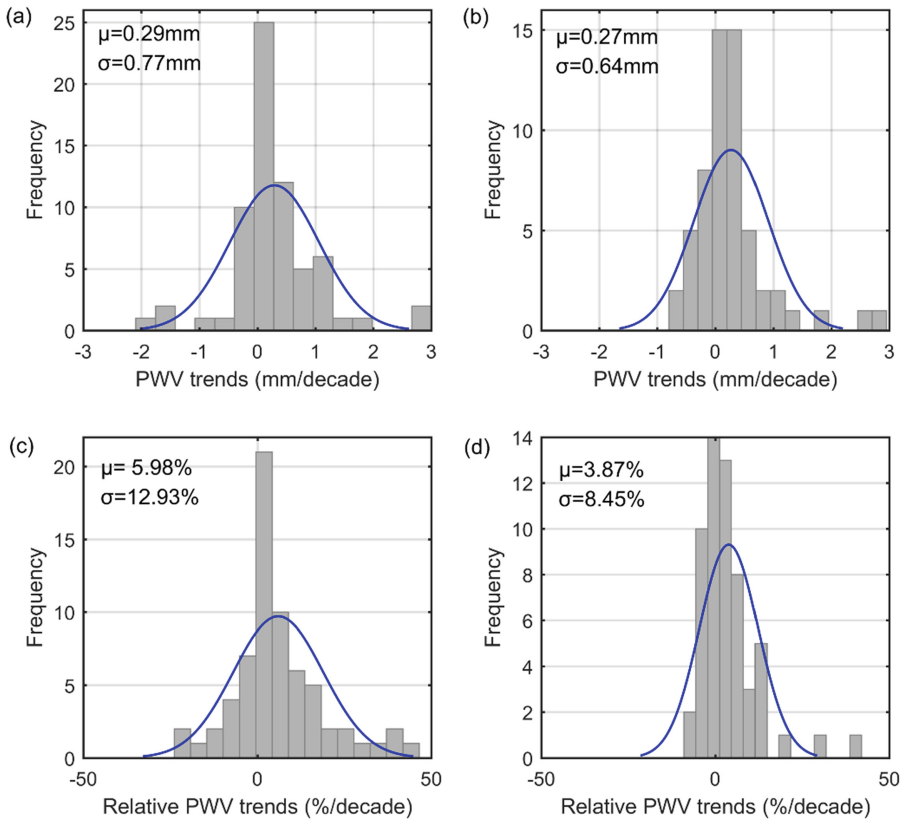

Fig. 6. Histogram of PWV trends and relative PWV trends of Antarctica and Greenland during 1994–2020.

To quantify more specifically the overall linear trend in Antarctica and Greenland, a histogram of the linear trend is plotted in Fig. 6 along with a Gaussian fit. From Fig. 6, it is known that the overall linear trends are 0.29 ± 0.77 mm and 0.27 ± 0.64 mm for Antarctica and Greenland, respectively, with relative linear trends of 5.98 ± 12.93%/decade and 3.87 ± 8.45%/decade, respectively. this indicates that (1) the overall trend of PWV is positive for both Antarctica and Greenland. This indicates that the PWV content at both poles has been increasing in the past two or more years; (2) the linear and relative linear trends are smaller overall for Greenland Island compared to Antarctica, and the differences between stations are also smaller, which means that the PWV is stronger overall for Greenland Island.

4 Conclusions

In this study, RS PWV and GNSS PWV for Antarctica and Greenland over the past two decades are counted and evaluated, and the spatial and temporal characteristics of PWV such as annual mean, standard deviation and interannual variability are analyzed and discussed, and the following conclusions are obtained:

(1) The multi-year mean values of PWV for Antarctica and Greenland are 5.63 ± 1.67 mm and 7.63 ± 1.35 mm, respectively, and the annual standard deviations of PWV are 1.60 ± 0.77 mm and 3.44 ± 0.92 mm, respectively.
(2) The annual STD of PWV showed a gradual increase from the land center to the edge in both Antarctica and Greenland; while the mean PWV decreased with increasing latitude in Greenland, and there was no significant latitudinal correlation in Antarctica.
(3) There is no significant regional difference in PWV liner trends, and from the statistical results, both Antarctica and Greenland show an increasing trend from year to year. The PWV trends were 0.29 ± 0.77 mm/decade and 0.27 ± 0.64 mm/decade for Antarctica and Greenland, respectively, with relative PWV trends of 5.98 ± 12.93%/decade and 3.87 ± 8.45%/decade, respectively.

Given that existing data are still sparse in the central regions of Antarctica and Greenland, increased efforts to establish more long-term PWV measurements in these regions are warranted.

References

1. Chahine, M.: The hydrological cycle and its influence on climate. Nature **359**(6394), 373 (1992)
2. Held, I., Soden, B.: Water vapor feedback and global warming. Annu. Rev. Energy Env. **25** (1), 441–475 (2000)
3. Lenderink, G., Van, M.: Increase in hourly precipitation extremes beyond expectations from temperature changes. Nat. Geosci. **1**(8), 511 (2008)
4. Sherwood, S., Roca, R., Weckwerth, T., et al.: Tropospheric water vapor, convection, and climate. Rev. Geophys. **48**(2) (2010)

5. Wagner, T., Beirle, S., Grzegorski, M., et al.: Global trends (1996 to 2003) of total column precipitable water observed by GOME on ERS-2 and their relation to surface temperature. J. Geophys. Res. Atmos. **111**(D12) (2006)
6. Zhou, T., Yu, R.: Atmospheric water vapor transport associated with typical anomalous summer rainfall patterns in China. J. Geophys. Res. Atmos. **110**(D8) (2005)
7. Zhao, C., Tie, X., Lin, Y.: Possible positive feedback of reduction of precipitation and increase in aerosols over eastern central China. Geophys. Res. Lett. **33**(11) (2006)
8. Allan, R., Soden, B.: Atmospheric warming and the amplification of precipitation extremes. Science **321**(5895), 1481–1484 (2008)
9. Luber, G., McGeehin, M.: Climate change and extreme heat events. Am. J. Prev. Med. **35**(5), 429–435 (2008)
10. Knapp, A., Beier, C., Briske, D., et al.: Consequences of more extreme precipitation regimes for terrestrial ecosystems. Bioscience **58**(9), 811–821 (2008)
11. Huang, Y., Cui, X.: Moisture sources of an extreme precipitation event in Sichuan, China, based on the Lagrangian method. Atmos. Sci. Lett. **16**(2), 177–183 (2015)
12. Serreze, M., Barrett, A., Stroeve, J.: Recent changes in tropospheric water vapor over the Arctic as assessed from radiosondes and atmospheric reanalyses. J. Geophys. Res. **117**, D10104 (2012)
13. Desser, A., Davis, S.: Trends in tropospheric humidity from reanalysis systems. J. Geophys. Res. Atmos. **115**(D19) (2010)
14. Zhang, L., Wu, L., Gan, B.: Modes and mechanisms of global water vapor variability over the twentieth century. J. Clim. **26**(15), 5578–5593 (2013)
15. Liu, N., Qin, J., Gao, Y., et al.: Trends and variability in atmospheric precipitable water over the Tibetan Plateau for 2000–2010. Int. J. Climatol. J. Royal Meteorol. Soc. (2015)
16. Dee, D., Rosnay, P., Uppala, et al.: The ERA-Interim reanalysis: configuration and performance of the data assimilation system. Q. J. Royal Meteorol. Soc. **137**(656), 553–597 (2011)
17. Wang, R., Fu, Y., Xian, T., et al.: Evaluation of atmospheric precipitable water characteristics and trends in Mainland China from 1995 to 2012. J. Clim. JCLI-D-16-0433.1 (2017)
18. Blewitt, G., Hammond, W., Kreemer, C.: Harnessing the GPS data explosion for interdisciplinary science. Eos. **99** (2018). https://doi.org/10.1029/2018EO104623
19. Zhang, F., Barriot, J., Xu, G., et al.: Metrology assessment of the accuracy of precipitable water vapor estimates from GPS data acquisition in tropical areas: the Tahiti case. Remote Sens. **10**(5), 758 (2018)
20. Wang, X., Zhu, W., Yan, H., et al.: Preliminary results of precipitable water vapor monitored by ground-based GPS. Chin. J. Atmos. Sci. **23**(5), 605–612 (1999)
21. Bevis, M., Businger, S., Herring, T., et al.: GPS meteorology: remote sensing of atmospheric water vapor using the global positioning system. J. Geophys. Res. **97**(D14), 15787–15801 (1992)